CHAPTER ELEVEN

Measuring the Energetic Coupling of Tertiary Contacts in RNA Folding using Single Molecule Fluorescence Resonance Energy Transfer

Max Greenfeld[*,†] *and* Daniel Herschlag[*,†]

Contents

Abstract

Tertiary contacts are critical to stabilizing the folded conformations of structured RNAs. In some cases, these contacts have been shown to interact with positive cooperativity. Measuring the energetic coupling of tertiary contact formation is among the most basic physical characterizations of a structured RNA. With proper experimental design, single-molecule fluorescence resonance energy transfer (smFRET) allows the rigorous determination of the energetic coupling. This chapter aims to provide a general experimental approach to measuring the energetic coupling of tertiary contacts, using smFRET.

* Department of Chemical Engineering, Stanford University, Stanford, California, USA
† Department of Biochemistry, Stanford University, Stanford, California, USA

Methods in Enzymology, Volume 472
ISSN 0076-6879, DOI: 10.1016/S0076-6879(10)72009-7

1. Introduction

Many RNAs have functions that require the formation of a well-defined tertiary structure, and new RNA structures are being solved at an exciting pace. These structures provide windows into the intricate conformations that RNAs can adopt. Dissecting the energetics of how a limited set of functional folded conformations is stabilized over the vast ensemble of unfolded or misfolded conformations remains central to understanding the fundamental physical properties of RNA (Cruz and Westhof, 2009; Li *et al.*, 2008; Noller, 2005).

Tertiary contacts are critical to maintaining the overall folds of structured RNAs. Yet dissecting the energetic coupling between the multiple tertiary contacts present in large structured RNAs has been difficult. While the thermodynamic contributions of individual tertiary contacts in stabilizing larger structured RNAs can have purely additive contributions or cooperative contributions, few measurements accurately determine these energetics. Measuring energetic coupling in RNA has been particularly challenging. This situation results from both experimental and conceptual difficulties that arise from RNA being a polyelectrolyte (Das *et al.*, 2005; Draper, 2004). In the limited case where an accurate quantitative measure of tertiary energetic coupling was determined, positive cooperativity was shown to provide a significant energetic contribution to folding (Sattin *et al.*, 2008).

Single-molecule fluorescence resonance energy transfer (smFRET) has been used to study conformations of a multitude of macromolecules, and some of the first applications were to structured RNAs (Ha *et al.*, 1999; Zhuang *et al.*, 2000). Currently, smFRET is a powerful and widely used tool in modern biophysics. Among the great strengths of smFRET is its ability to directly measure equilibria over a large dynamic range. This property enables RNA molecules with substantial differences in stabilities to be compared in solutions with identical ionic composition. This ability circumvents spurious assumptions made when using a Hill analysis to assess RNA energetics (Das *et al.*, 2005; Draper, 2004). The application of smFRET for measuring tertiary contact cooperativity in the P4-P6 domain of the *Tetrahymena* Group I intron (P4-P6) provided the first accurate measurement of positive cooperativity in P4-P6 folding and revealed that cooperativity depends on the ionic conditions (Sattin *et al.*, 2008). Although this was the first measurement of RNA cooperativity using smFRET, the approach taken does not rely on the details of P4-P6 as a model system.

This chapter provides a general approach to measuring the energetic coupling of tertiary contacts in structured RNAs. We first introduce the types of energetic couplings that can occur and explain why most techniques do not provide accurate thermodynamic measures of these energetics.

The use of smFRET as a general technique for accurately measuring the coupling in tertiary contacts is then presented. As there are multiple methods available for making RNA constructs suitable for smFRET and multiple strategies for measuring smFRET, references to other resources are provided for those details. Discussion instead focuses on the steps that are required for making meaningful energetic comparisons.

2. Thermodynamic Cooperativity Overview

Among the most basic characterization of any macromolecular binding or conformational change is determination of the equilibrium constant of that event. However, a single-equilibrium constant does not give mechanistic insight into the complex reaction being studied. A more complete thermodynamic understanding of a complex equilibrium can often be obtained by dividing the reaction into smaller discrete equilibria. The parsing of a complex equilibrium has two primary aims: (1) to identify the energetic importance of observed structural interactions and (2) to evaluate how smaller discrete energetic components combine to contribute to the overall equilibrium of a reaction. The latter aim is the focus of this chapter.

When the free energy of a complex chemical equilibrium is evaluated by measuring the free energy of simpler components, the individual components might or might not sum to the overall free energy. The question of whether the energetic components of a particular equilibrium are additive or cooperative is a recurring question in macromolecule studies. A particularly lucid discussion of how energetic components relate to the overall energetics is presented in the classic paper by Jencks (1981).

The basic approach to measuring the energetic coupling of a reaction is shown in Fig. 11.1. In this generic thermodynamic diagram, $K_{overall}$ is the

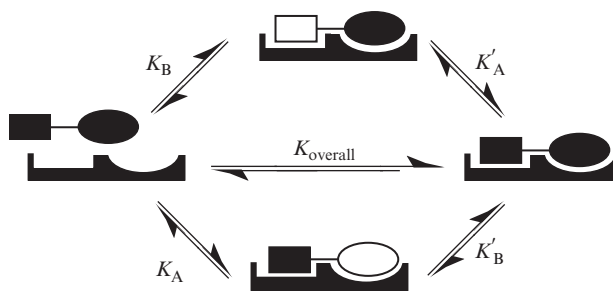

Figure 11.1 Generic thermodynamic cycle for assessing cooperativity of two binding sites. In the case of RNA folding, the square and oval would represent two distinct tertiary contacts, filled shapes are indicative of native tertiary contacts, while the outlines only are indicative of ablated tertiary contacts. Figure adapted from Jencks (1981).

overall equilibrium constant. The overall reaction can be broken into four distinct equilibria, K_A, K'_A, K_B, and K'_B, representing the piecewise completion of the overall reaction. The question becomes, how do the free energies of the individual reaction steps compare to one another. As shown in Fig. 11.2, there are three possible ways in which the thermodynamic cycle of Fig. 11.1 can be completed. In the case of no cooperativity (i.e., energetic additivity), there is no free energy difference depending on the order in which the tertiary contacts are formed ($\Delta G_a = \Delta G'_a$ and $\Delta G_b = \Delta G'_b$). In the case of positive cooperativity, the free energy gained upon formation of the second contact is greater than if the same contact were formed first ($\Delta G_a > \Delta G'_a$ and $\Delta G_b > \Delta G'_b$). And in the case of negative cooperativity, the free energy gained upon formation of the second contact is less than if the same contact were formed first ($\Delta G_a < \Delta G'_a$ and $\Delta G_b < \Delta G'_b$).

It is convenient to express the relationships depicted in the free energy diagram of Fig. 11.2 by Eq. (11.1).

$$\Delta G_{coop} = -RT \ln \frac{K'_A}{K_A} = -RT \ln \frac{K'_B}{K_B}. \tag{11.1}$$

This representation highlights that ΔG_{coop} is a function solely arising from the order of contact formation. Whereas ΔG_{coop} is a measurement that can be made for diverse systems, the actual value and mechanistic origins can vary greatly (Mammen *et al.*, 1998; Williamson, 2008).

In practice, there are many considerations that arise when trying to experimentally realize the thermodynamic diagram in Fig. 11.1. Most basically,

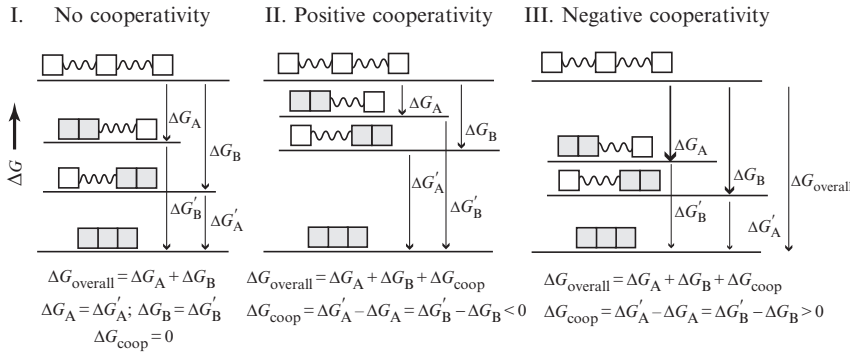

Figure 11.2 Free energy diagram indicating the possible solutions of the thermodynamic cycle in Fig. 11.1. (I) No cooperativity arises when the sum of the free energies of each individual contact is equal to the overall free energy. (II) Positive cooperativity arises when the overall free energy is greater than the sum of the individual components. (III) Negative cooperativity arises when the overall free energy is less than the sum of the individual components.

cleanly ablating contacts that maintain well-defined intermediate conformations can be difficult, and measurements of K'_A and K'_B can be difficult or impossible, so ΔG_{coop} is usually calculated in terms of $K_{overall}$, as shown in Eq. (11.2).

$$\Delta G_{coop} = -RT \ln \frac{K_{overall}}{K_A K_B}. \tag{11.2}$$

Even rigorous measurement of $K_{overall}$, K_A, and K_B can be difficult. Dealing with each of these measurements is critical to successfully measuring cooperativity in RNA folding.

3. Measuring Folding Equilibrium in RNA

Each RNA residue has a formal negative charge so that any RNA more than a few residues in length is a polyelectrolyte. It has been estimated that the columbic repulsion, in the absence of counterions, upon folding of the approximately 400-nucleotide *Tetrahymena* Group I intron is 10^3 kcal/mol (Bai *et al.*, 2005). However, RNA in solution always exists in the presence of counterions that form an ion atmosphere surrounding the molecule (Bai *et al.*, 2007). These counterions attenuate the electrostatic repulsion arising from the phosphate backbone and consequently affect the stability of the folded and unfolded states (Das *et al.*, 2005; Draper, 2004; Grilley *et al.*, 2006).

Making correct energetic measurements of RNA requires comparisons of equilibria under identical ionic conditions. Models that assume only specific ion-binding stoichiometries are not energetically correct, as is extensively discussed elsewhere (Das *et al.*, 2005; Draper, 2004). It is possible to measure the equilibrium of an RNA molecule by titrating a solution component (e.g., Mg^{2+}), monitoring a variable such as the radius of gyration or the protection of a tertiary contact from chemical modification, and fitting the results assuming a two-state model. However, RNA folding is not, in general, two state in nature, and there is limited accuracy of empirical extrapolations away from the well-determined midpoints of such sigmoidal curves. These limitations prevent accurate energetic comparisons of molecules with significantly different folding midpoints.

The limitations associated with typical methods of determining an RNA folding equilibrium can be overcome with smFRET. Many RNAs that have been examined with smFRET have a FRET signal that is dominated by a single high-FRET and single-low-FRET state. This clear distinction of states allows the direct measurement of the equilibrium constant of a molecule without extrapolation or assumptions of a two-state model. Moreover, smFRET is accurate over a wide dynamic range and is hence

suitable for comparing molecules with large stability differences. Despite these advantages, the time required to set up and conduct smFRET measurements should be considered before initiating the measurements highlighted in this chapter.

4. Designing an smFRET Experiment to Measure Cooperativity

The precipitous rise in smFRET publications is inevitably related to the relative ease with which smFRET experiments can be designed and measurements carried out (Joo *et al.*, 2008). Indeed, it is possible for an investigator without a specialized interest in smFRET to design and carry out an enlightening set of experiments. And although interpreting smFRET measurements requires careful experimental design at multiple steps and successful completion of these steps can be difficult, the added insight of smFRET experiments can be well worth the effort.

Experimental measurement of the energetic coupling of tertiary contacts in RNA requires realizing the thermodynamic scheme in Fig. 11.1 for an actual RNA. Figure 11.3 highlights the five major steps that were required for measuring tertiary contact cooperativity in the P4-P6 domain of the *Tetrahymena* Group I ribozyme. The discrete structure of RNA tertiary contacts suggests that there is nothing unique to P4-P6 that enabled the measurements by Sattin *et al.* (2008).

This section details the experimental approaches and decisions that must be made during each of the five steps in Fig. 11.3. There were a number of key controls and design choices that were necessary for the measurements made by Sattin *et al.* (2008) that will be required for most if not all structured RNAs studied in an analogous fashion. The methods presented are biased by the experimental decisions that were successful in the approaches taken to measure P4-P6 tertiary contact cooperativity, but the aim of this section is to present the general experimental design process. Wherever possible, alternative approaches, controls, and methods are discussed.

4.1. Identification of tertiary contacts

There are multiple ways in which tertiary contacts can be identified in a structured RNA. Phylogenetic analysis, chemical footprinting, site-directed mutagenesis, and crystallography have all been used to identify or confirm the presence and location of tertiary contacts. In practice, the first two methods are synergistic and common for identifying tertiary contacts. The increased proficiency with which RNAs can be crystallized can more commonly provide aid in the design of smFRET experiments. However, high-resolution structural

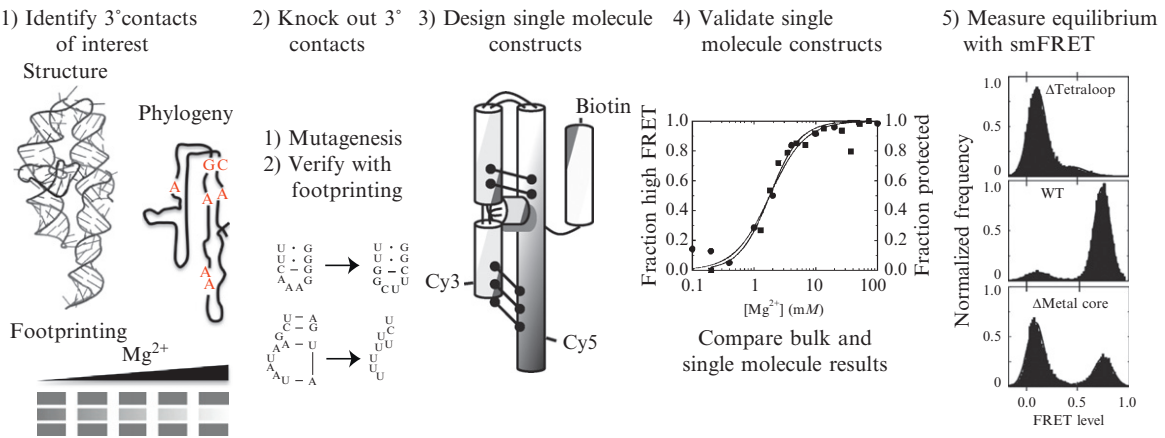

Figure 11.3 Key steps required to measure tertiary contact cooperativity in RNA using smFRET. (1) Use the available structural information to identify the key tertiary contacts of interest. (2) Make constructs that knock out the tertiary contacts of interest. (3) Construct the wild type and two tertiary contact mutant molecules with FRET pairs and surface attachment. (4) Verify the single molecule constructs recapitulate the expected behavior of the unlabeled molecules. (5) Directly determine the equilibrium of the molecules under identical ionic conditions.

information is not required. Additionally, it is not necessary to identify all of the tertiary contacts in an RNA. The smFRET technique can be used for the rigorous thermodynamic characterization of any two contacts that influence the same conformational change.

4.2. Knocking out tertiary contacts

Constructing mutant RNAs that have the tertiary contacts of interest knocked out is straightforward. Point mutations of highly conserved residues or key contacts observed in crystal structures are particularly good targets to mutate. Alternatively, simply changing a few residues to uridines, base pairing, or deleting bulged residues in a tertiary contact is usually sufficient to knock out the contact.

It is important to assess the effects of mutations on the overall fold of the RNA. It is possible to make tertiary contact mutations that weaken and do not completely ablate the tertiary contacts. Alternatively, it is possible that the mutation is so severe that multiple tertiary contacts are affected simultaneously. Therefore, it is important to verify with a technique like chemical footprinting that the contacts have been locally removed (Takamoto *et al.*, 2004). It is also valuable to compare the effects of multiple mutations aimed to knock out the same interaction. The limitations of site-directed mutagenesis will affect the interpretation of downstream energetic measurements, so it is important to have multiple strains of evidence that define the behavior of all molecules being studied.

4.3. Designing single molecule constructs

Nucleic acids have been among the most amenable molecules for study by single-molecule spectroscopy. This fact arises for a number of reasons. There are vast and accessible synthetic resources for constructing modified nucleotides. Watson/Crick base pairing rules at times allow for the rational engineering of simple molecular structure. And an underappreciated advantage is that nucleic acids are less prone to nonspecific surface absorption than are proteins. Taken together, these properties provide significant flexibility and creativity with the design and construction of RNAs for single-molecule spectroscopy.

When designing an RNA construct for study with smFRET, there are three major design considerations: (1) the location of the donor and acceptor fluorophore; (2) the specific FRET pair to be used (e.g., Cy3-Cy5) and the method of fluorophore incorporation; and (3) the location of the surface tether and the choice of attachment method. There is no *a priori* method for sorting through all the possibilities of the three steps. Indeed at the beginning of a project, it is advisable to try multiple strategies with the intent of

narrowing the possibilities once the utility of each is tested in a specific system.

The choice of dye location is most critical to downstream quantification and interpretation of the measured FRET signal. The FRET pairs should be placed in locations that monitor a conformational change mediated by the two tertiary contacts being studied. Although techniques sensitive to the unfolded structure of an RNA such as SAXS or native gels can be used to infer the major conformational changes, they do not identify positions for labeling that are far apart in the unfolded state and nonperturbing in the folded state. Crystal structures and footprinting studies provide useful information for this design. Ideally, the locations should be chosen to maximize the difference between the high- and low-FRET values of the conformational change being monitored and to not interfere with important structural interactions.

In the case of P4-P6, detailed structural information provided significant constraints on the location of FRET pairs (just above the tetraloop and just below the tetraloop receptor). This placement monitors a large conformational change mediated by a hinge region distal to the FRET pairs and the two tertiary contacts in P4-P6. The specific location of the dyes, at the level of a single nucleotide, was determined by the structural information and the constraints of the labeling scheme used.

In most cases, fluorophores are attached to an RNA by derivatizing a primary amino group. This approach requires specifically incorporating a modified base or a terminal amino modified linker. There are a number of commercially available fluorophores that are commonly used in smFRET studies. A current summary of the commonly used dyes is included in Table 11.1 of Roy *et al.* (2008). As new fluorophores become commercially available this list will grow. Currently, there are four methods available for site-specifically modifying RNAs, and these methods and their strengths and limitations are listed in Table 11.1 herein.

Table 11.1 Strategies for incorporating FRET pairs into RNA

	Minimal perturbation	Length limitation	Covalent attachment	Many steps
Fully synthetic RNA	Yes	~50 nt	Yes	No
Splinted ligation	Yes	No	Yes	Yes
Base pairing	No	No	No	No
2′-OH ligation	No	No	Yes	No

Using fully synthetic RNA is the easiest method for making single-molecule constructs (Hodak *et al.*, 2005; Pereira *et al.*, 2008; Tan *et al.*, 2003; Zhuang *et al.*, 2002). Indeed if dyes are to be placed on the 5′- or 3′-end of an RNA, it is possible to purchase molecules with the dyed attached during synthesis, eliminating the need to postsynthetically label the RNA. However, there are considerable length limitations with fully synthetic RNAs. The use of ligation to introduce short synthetic RNAs, which can be derivatized with a fluorophore prior to incorporation into the complete RNA, removes the length limitation of using fully synthetic RNAs. This technique is gaining in prevalence, although it can be time consuming to implement (Akiyama and Stone, 2009; Sattin *et al.*, 2008; Solomatin and Herschlag, 2009; Stone *et al.*, 2007). The use of base-pairing rules to hybridize fluorescently labeled oligonucleotides to 5′- or 3′-extensions of an RNA or to loop structures have been used successfully in a number of cases (Dorywalska *et al.*, 2005; Smith *et al.*, 2005, 2008; Zhuang *et al.*, 2000). Despite the potential ease of this approach, extensions are restricted to the ends of RNAs and hybridization to internal loops can perturb the RNA's structure. Finally, a method has recently been introduced for site-specifically ligating an RNA oligonucleotide to the 2′-OH of adenosines in an RNA sequence (Baum and Silverman, 2007). This technique has not yet been used for smFRET studies. If the rather bulky labels tend not to perturb the molecules, as suggested by the initial study, this technique could have broad applications.

The choice of labeling methods will largely depend on the molecule being studied. For instance, the design of P4-P6 for smFRET studies required all three of the available techniques to be considered at the time. More information is provided in recent *Methods in Enzymology* chapters (Akiyama and Stone, 2009; Solomatin and Herschlag, 2009).

Compared with the first two design steps, there are a limited set of choices in the position and location of the surface tether. To the best of the authors' knowledge, a biotin/streptavidin linkage has been used universally as the final surface attachment in smFRET studies of nucleic acids. Alternative schemes such as incorporating an RNA-binding protein motif into an RNA and using a surface derivatized with the RNA-binding protein could be practical in some situations, such as very large RNAs but has yet to be implemented. To rule out the potential of surface affects, molecules have been confined in tethered lipid vesicles (Boukobza *et al.*, 2001; Okumus *et al.*, 2004). This approach is typically used as a secondary attachment scheme for a limited set of control experiments. However, it could be used to avoid the need to design a covalently attached surface tether in an RNA construct.

Surface tethers are typically placed at the 5′- or 3′-end of an RNA. If synthetic RNA is used on either the 5′- or 3′-end of an RNA, a terminal biotin-derivatized base can be incorporated for surface attachment. Alternatively, tails of extra bases, typically 20–30 nucleotides, can be incorporated.

In this situation, a biotin-derivatized oligonucleotide complementary to the tail can be used for surface attachment. A potential advantage of using a 5′- or 3′-tail is that there is space between the fluctuating RNA and the site of attachment. However, the ease of direct covalent attachment of the biotin has been used without trouble by a number of investigators. It should also be noted that RNA can be internally labeled with biotin, either during synthesis or via ligation to the 2′-OH, although these strategies have not seen use in smFRET studies.

4.4. Validating a new single-molecule construct

Gaining expertise with the instrumentation required for carrying out smFRET measurements is an involved process and has been discussed elsewhere (Joo and Ha, 2008; Roy *et al.*, 2008). The confidence with which a new construct can be validated is dependent on past successes. It is important for an experimentalist to validate their protocols by redetermining kinetic and thermodynamic properties of molecules that have been previously studied. There are many variables that affect the quality of an smFRET measurement, only one of which is the intrinsic behavior of the molecule being studied. Trouble in reproducing values could result from technical differences such as poor signal-to-noise, short trace length or different criteria for analyzing molecules. If differences arise, it is necessary to resolve the discrepancies.

There is significant variability in the behavior of single-molecule constructs. Figure 11.4A shows a trace of wild-type P4-P6, which by standard measures is a well-behaved molecule. P4-P6 has stable high- and low-FRET states that do not change with time. The FRET pairs monitor a large conformational change, which provides significant separation between the high- and low-FRET states. And under the correct experimental conditions (Sattin *et al.*, 2008), P4-P6 produces traces with high signal-to-noise and long lifetimes. However, this behavior cannot be expected of all molecules. Mutations that significantly destabilize the folded conformation are likely to produce poorer quality traces. This is the case with the tetraloop knockout of P4-P6, which has the lowest stability of the three constructs being compared and has a different high-FRET state value than the wild type and metal core knockout (Fig. 11.4B). In the case of P4-P6, the FRET difference was consistent with conformational changes known to occur in the P5abc region of the molecule. For P4-P6, having an understanding of why the high-FRET value changed for one of the constructs was important for ensuring that the correct conformations were being monitored. Alternatively, concerns that the mutations were significantly altering the folded conformations would persist, undermining the assumptions required of the thermodynamic diagram in Fig. 11.1.

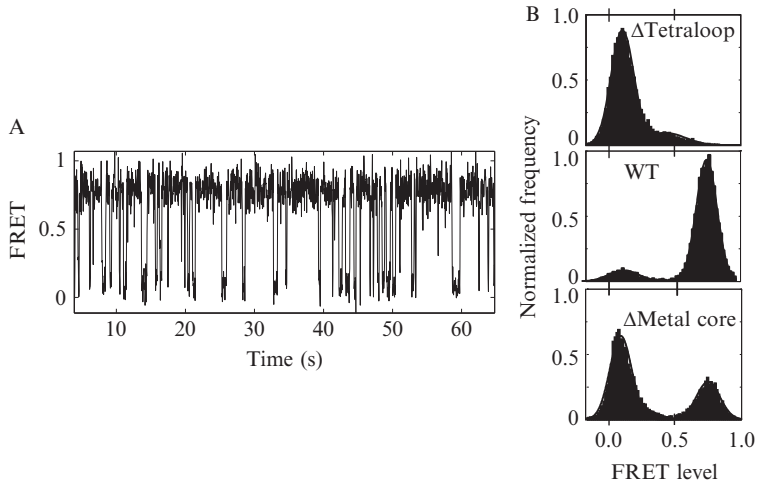

Figure 11.4 Characteristic data from the measurement of P4-P6 cooperativity. (A) Representative trace for WT P4-P6. P4-P6 has well-defined high- and low-FRET states. Using wide field imaging on a custom built prism based total internal reflection fluorescence microscope (see Bartley *et al.*, 2003; Zhuang *et al.*, 2000 for description), a high signal-to-noise of ~4 and stable donor and acceptor intensities are obtainable for traces well over 1 min. (B) Cumulative FRET histograms for hundreds of molecules of each construct. Histograms indicate the molecules can be thermodynamically described with two states. As such the equilibrium is the ratio of the areas under the two peaks in the FRET histograms. Panel (B) reprinted with permission from Sattin *et al.* (2008).

The most basic quantitative analysis of smFRET measurements is the determination of a cumulative FRET histogram. Examples of these are shown for the wild type and two mutant forms of P4-P6 in Fig. 11.4B. This analysis simply involves making a histogram of FRET traces from many molecules (typically hundreds). In most cases, the histogram consists of two peaks that are well fitted by a Gaussian distribution (an approximation since FRET values outside the range of 0–1 have no physical meaning—the actual peak shapes are governed by the β-distribution (McKinney *et al.*, 2006)). If this is not the case and there are more than two equilibrium states of the molecule being studied, the analysis of cooperativity is valid only if changes in the distributions are limited to two of the peaks. The equilibrium between any two peaks is simply the ratio of the area of the two peaks as given by Eq. (11.3)

$$K_{\text{overall}} = \frac{A_{\text{FRET}}^{\text{High}}}{A_{\text{FRET}}^{\text{Low}}}, \tag{11.3}$$

where K_{overall} is the equilibrium constant, $A_{\text{FRET}}^{\text{High}}$ area of the high-FRET peak, and $A_{\text{FRET}}^{\text{Low}}$ is the area of the low-FRET peak.

Analysis of single-molecule data can be immensely complex because of the heterogeneity that is revealed by removing ensemble averaging. Almost every RNA that has been studied with smFRET has demonstrated this complex underlying behavior, making it quite likely that any new constructs will behave analogously. Although the molecular origins of this type of behavior remain largely unexplained (Ditzler *et al.*, 2008; Huang *et al.*, 2009; Korennykh *et al.*, 2007), the analysis of heterogeneity has recently become experimentally tractable (Elenko *et al.*, 2009; Solomatin *et al.*, 2010). Fortunately, the measurement of cooperativity is a strictly thermodynamic measurement that assumes that all molecules are covalently identical and unperturbed by the surface or dyes. In this instance, heterogeneity should not affect the results. For P4-P6, it was possible to test this assumption by comparing the equilibrium behavior of P4-P6 determined by smFRET to that determined by bulk hydroxyl radical footprinting (see the supplemental information of Sattin *et al.* (2008)). The fact that the two measurements matched well was an important validation of the accuracy of the cooperativity measurement.

4.5. Measurement of cooperativity

At the successful completion of the first four steps, the actual equilibrium measurements are straightforward. The only strict requirement is that the three-way comparisons between the two mutant and wild-type molecules be made under identical ionic conditions. For P4-P6, a number of different ionic conditions were attempted before finding a single condition where the equilibrium constant for each of the molecules could be accurately determined. Some searching for conditions where accurate measurements are made can be expected for other constructs. Once measurements are made, the thermodynamic cycle shown in Fig. 11.1 can be completed using Eqs. (11.1) and (11.2). The results of the previous P4-P6 analysis are shown in Fig. 11.5. The measured ΔG_{coop} of -2.3 kcal/mol (note that the sign is consistent with the convention used here) likely plays a significant role in stabilizing the folded structure of P4-P6. This value differs significantly from less rigorous measurements, affirming the importance of smFRET as a technique for correctly measuring cooperativity in RNA tertiary structure.

5. Additional Comments

The generality with which smFRET can be used to measure the energetic coupling of RNA tertiary contacts should provide an important tool for the study of RNA structure. In addition to extending cooperativity measurements to RNAs other than P4-P6, future work will hopefully give

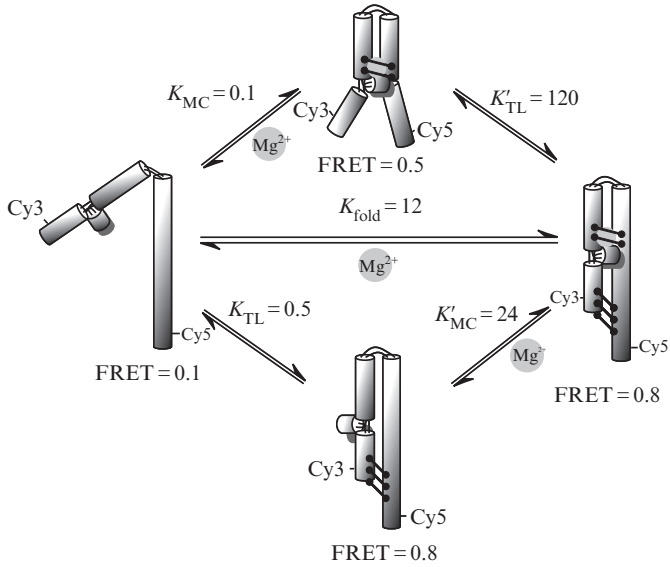

Figure 11.5 Thermodynamic cycle for tertiary contact cooperativity in P4-P6. The cooperativity was measured to be -3.2 ± 0.2 kcal/mol in 10 m*M* Mg^{2+}, 200 m*M* NaCl, 50 m*M* Na-MOPS, pH 7.0, and 22 °C. Reprinted with permission from Sattin *et al*. (2008).

insight to the influence of the ionic conditions and the mechanistic implications of heterogeneity on cooperativity.

As further measurements are made on different RNAs and under increasingly diverse ionic conditions, it is likely that interpretable trends will arise and new properties suggested. Already with P4-P6, it is clear that cooperativity depends on the ionic conditions, which is an additional energetic coupling that is not yet understood.

Heterogeneity as observed by smFRET suggests the presence of long-lived conformational differences among RNA molecules. The possibility of measuring cooperativity differences among conformationally distinct structures is an exciting and uniquely single-molecule measurement. It will be a worthy experimental challenge to develop a model system where the thermodynamic diagram in Fig. 11.1 can be recapitulated for a single molecule in a distinct conformational state.

We hope that this chapter provides some insight into the experimental details important for a thorough analysis of smFRET cooperativity measurements. There are certainly many additional opportunities for smFRET to provide detailed biophysical insight into RNA structure. Considering the significant insights already provided, it seems likely that this technique will expand our current understanding of RNA biophysics and contribute insights into the complex functions carried out by RNA.

ACKNOWLEDGMENTS

We thank Bernie D. Sattin for help in preparing the figures. Funding was provided by NIH program project grant P01-GM-66275 to D. H.

REFERENCES

Akiyama, B. M., and Stone, M. D. (2009). Assembly of complex RNAs by splinted ligation. *Methods Enzymol.* **469,** 27–46.

Bai, Y., Das, R., Millett, I., Herschlag, D., and Doniach, S. (2005). Probing counterion modulated repulsion and attraction between nucleic acid duplexes in solution. *Proc. Natl. Acad. Sci. USA* **102,** 1035–1040.

Bai, Y., Greenfeld, M., Travers, K. J., Chu, V. B., Lipfert, J., Doniach, S., and Herschlag, D. (2007). Quantitative and comprehensive decomposition of the ion atmosphere around nucleic acids. *J. Am. Chem. Soc.* **129,** 14981–14988.

Bartley, L. E., Zhuang, X. W., Das, R., Chu, S., and Herschlag, D. (2003). Exploration of the transition state for tertiary structure formation between an RNA helix and a large structured RNA. *J. Mol. Biol.* **328,** 1011–1026.

Baum, D. A., and Silverman, S. K. (2007). Deoxyribozyme-catalyzed labeling of RNA. *Angew. Chem. Int. Ed.* **46,** 3502–3504.

Boukobza, E., Sonnenfeld, A., and Haran, G. (2001). Immobilization in surface-tethered lipid vesicles as a new tool for single biomolecule spectroscopy. *J. Phys. Chem. B* **105,** 12165–12170.

Cruz, J. A., and Westhof, E. (2009). The dynamic landscapes of RNA architecture. *Cell* **136,** 604–609.

Das, R., Travers, K. J., Bai, Y., and Herschlag, D. (2005). Determining the Mg^{2+} stoichiometry for folding an RNA metal ion core. *J. Am. Chem. Soc.* **127,** 8272–8273.

Ditzler, M. A., Rueda, D., Mo, J. J., Hakansson, K., and Walter, N. G. (2008). A rugged free energy landscape separates multiple functional RNA folds throughout denaturation. *Nucleic Acids Res.* **36,** 7088–7099.

Dorywalska, M., Blanchard, S. C., Gonzalez, R. L., Kim, H. D., Chu, S., and Puglisi, J. D. (2005). Site-specific labeling of the ribosome for single-molecule spectroscopy. *Nucleic Acids Res.* **33,** 182–189.

Draper, D. E. (2004). A guide to ions and RNA structure. *RNA* **10,** 335–343.

Elenko, M. P., Szostak, J. W., and van Oijen, A. M. (2009). Single-molecule imaging of an in vitro-evolved RNA aptamer reveals homogeneous ligand binding kinetics. *J. Am. Chem. Soc.* **131,** 9866–9867.

Grilley, D., Soto, A. M., and Draper, D. E. (2006). Mg^{2+}-RNA interaction free energies and their relationship to the folding of RNA tertiary structures. *Proc. Natl. Acad. Sci. USA* **103,** 14003–14008.

Ha, T., Zhuang, X. W., Kim, H. D., Orr, J. W., Williamson, J. R., and Chu, S. (1999). Ligand-induced conformational changes observed in single RNA molecules. *Proc. Natl. Acad. Sci. USA* **96,** 9077–9082.

Hodak, J. H., Fiore, J. L., Nesbitt, D. J., Downey, C. D., and Pardi, A. (2005). Docking kinetics and equilibrium of a GAAA tetra loop-receptor motif probed by single-molecule FRET. *Proc. Natl. Acad. Sci. USA* **102,** 10505–10510.

Huang, Z., Pei, W. M., Han, Y., Jayaseelan, S., Shekhtman, A., Shi, H., and Niu, L. (2009). One RNA aptamer sequence, two structures: A collaborating pair that inhibits ampa receptors. *Nucleic Acids Res.* **37,** 4022–4032.

Jencks, W. P. (1981). On the attribution and additivity of binding-energies. *Proc. Natl. Acad. Sci. USA* **78,** 4046–4050.

Joo, C., and Ha, T. (2008). Single-molecule FRET with total internal reflection microscopy. *Single Molecule Techniques: A Laboratory Manual* pp. 3–36.

Joo, C., Balci, H., Ishitsuka, Y., Buranachai, C., and Ha, T. (2008). Advances in single-molecule fluorescence methods for molecular biology. *Annu. Rev. Biochem.* **77,** 51–76.

Korennykh, A. V., Plantinga, M. J., Correll, C. C., and Piccirilli, J. A. (2007). Linkage between substrate recognition and catalysis during cleavage of sarcin/ricin loop RNA by restrictocin. *Biochemistry* **46,** 12744–12756.

Li, P. T. X., Vieregg, J., and Tinoco, I. (2008). How RNA unfolds and refolds. *Annu. Rev. Biochem.* **77,** 77–100.

Mammen, M., Choi, S. K., and Whitesides, G. M. (1998). Polyvalent interactions in biological systems: Implications for design and use of multivalent ligands and inhibitors. *Angew. Chem. Int. Ed.* **37,** 2755–2794.

McKinney, S. A., Joo, C., and Ha, T. (2006). Analysis of single-molecule FRET trajectories using hidden Markov modeling. *Biophys. J.* **91,** 1941–1951.

Noller, H. F. (2005). RNA structure: Reading the ribosome. *Science* **309,** 1508–1514.

Okumus, B., Wilson, T. J., Lilley, D. M. J., and Ha, T. (2004). Vesicle encapsulation studies reveal that single molecule ribozyme heterogeneities are intrinsic. *J. Phys. Chem. B* **87,** 2798–2806.

Pereira, M. J. B., Nikolova, E. N., Hiley, S. L., Jaikaran, D., Collins, R. A., and Walter, N. G. (2008). Single vs ribozyme molecules reveal dynamic and hierarchical folding toward catalysis. *J. Mol. Biol.* **382,** 496–509.

Roy, R., Hohng, S., and Ha, T. (2008). A practical guide to single-molecule FRET. *Nat. Methods* **5,** 507–516.

Sattin, B., Zhao, W., Travers, K., Chut, S., and Herschlag, D. (2008). Direct measurement of tertiary contact cooperativity in RNA folding. *J. Am. Chem. Soc.* **130,** 6085–6087.

Smith, G. J., Sosnick, T. R., Scherer, N. F., and Pan, T. (2005). Efficient fluorescence labeling of a large RNA through oligonucleotide hybridization. *RNA* **11,** 234–239.

Smith, G. J., Lee, K. T., Qu, X. H., Xie, Z., Pesic, J., Sosnick, T. R., Pan, T., and Scherer, N. F. (2008). A large collapsed-state RNA can exhibit simple exponential single-molecule dynamics. *J. Mol. Biol.* **378,** 943–953.

Solomatin, S., and Herschlag, D. (2009). Methods of site-specific labeling of RNA with fluorescent dyes. *Methods Enzymol.* **469,** 47–68.

Solomatin, S. V., Greenfeld, M., Chu, S., and Herschlag, D. (2010). Multiple native states reveal persistent ruggedness of an RNA folding landscape. *Nature* **463,** 681–684.

Stone, M. D., Mihalusova, M., O'Connor, C. M., Prathapam, R., Collins, K., and Zhuang, X. W. (2007). Stepwise protein-mediated RNA folding directs assembly of telomerase ribonucleoprotein. *Nature* **446,** 458–461.

Takamoto, K., Das, R., He, Q., Doniach, S., Brenowitz, M., Herschlag, D., and Chance, M. R. (2004). Principles of RNA compaction: Insights from the equilibrium folding pathway of the P4-P6 RNA domain in monovalent cations. *J. Mol. Biol.* **343,** 1195–1206.

Tan, E., Wilson, T. J., Nahas, M. K., Clegg, R. M., Lilley, D. M. J., and Ha, T. (2003). A four-way junction accelerates hairpin ribozyme folding via a discrete intermediate. *Proc. Natl. Acad. Sci. USA* **100,** 9308–9313.

Williamson, J. R. (2008). Cooperativity in macromolecular assembly. *Nat. Chem. Biol.* **4,** 458–465.

Zhuang, X. W., Bartley, L. E., Babcock, H. P., Russell, R., Ha, T. J., Herschlag, D., and Chu, S. (2000). A single-molecule study of RNA catalysis and folding. *Science* **288,** 2048–2051.

Zhuang, X. W., Kim, H., Pereira, M. J. B., Babcock, H. P., Walter, N. G., and Chu, S. (2002). Correlating structural dynamics and function in single ribozyme molecules. *Science* **296,** 1473–1476.